Effects of Hypoxia-Induced Gill Remodelling on the Innervation and Distribution of Ionocytes in the Gill of Goldfish, *Carassius auratus*

Velislava Tzaneva, Claudia Vadeboncoeur, Jaimee Ting, and Steve F. Perry*

Department of Biology, University of Ottawa, Ottawa, Ontario, K1N 6N5, Canada

ABSTRACT

The presence of an interlamellar cell mass (ILCM) on the gills of goldfish acclimated to 7°C leads to preferential distribution of branchial ionocytes to the distal edges of the ILCM, where they are likely to remain in contact with the water and hence remain functional. Upon exposure to hypoxia, the ILCM retracts, and the ionocytes become localized to the lamellar surfaces and on the filament epithelium, owing to their migration and the differentiation of new ionocytes from progenitor cells. Here we demonstrate that the majority of the ionocytes receive neuronal innervation, which led us to assess the consequences of ionocyte migration and differentiation during hypoxic gill remodelling on the pattern and extent of ionocyte neuronal innervation. Normoxic 7°C goldfish (ILCM present) possessed significantly greater numbers of ionocytes/ mm^2 (951.2 $\pm$ 94.3) than their 25°C conspecifics (ILCM absent; 363.1 $\pm$ 49.6) but a statistically lower percentage of innervated ionocytes (83.1% $\pm$ 1.0% compared with 87.8% $\pm$ 1.3%). After 1 week of exposure of goldfish to hypoxia, the pool of branchial ionocytes was composed largely of pre-existing migrating cells (555.6 $\pm$ 38.1/mm^2) and to a lesser extent newly formed ionocytes (226.7 $\pm$ 15.1/mm^2). The percentage of new (relative to pre-existing) ionocytes remained relatively constant (at $\sim$30%) after 1 or 2 weeks of normoxic recovery. After hypoxia, pre-existing ionocytes expressed a greater percentage of innervation than newly formed ionocytes in all treatment groups; however, their percentage innervation steadily decreased over 2 weeks of normoxic recovery. J. Comp. Neurol. 522:118–130, 2014.

© 2013 Wiley Periodicals, Inc.

INDEXING TERMS: ILCM; hypoxia; gill remodelling; gill epithelia

---

The goldfish (*Carassius auratus*) exhibits structural modifications to its gills in response to changes in water temperature, O$_2$ levels, or exercise (Sollid et al., 2005; Mitrovic et al., 2009; Mitrovic and Perry, 2009; Tzaneva et al., 2011; Fu et al., 2011; Perry et al., 2012). At colder temperatures (<15°C), the functional lamellar surface area is decreased by the growth of a cell mass between the lamellae which has been termed the *interlamellar cell mass* (ILCM; Sollid et al., 2003). The ILCM is shed when the fish is exposed to hypoxia (Sollid et al., 2005; Mitrovic et al., 2009; Tzaneva et al., 2011) or warmer water temperatures (>15°C; Mitrovic and Perry, 2009) or during forced aerobic exercise (Fu et al., 2011; Perry et al., 2012). The process of ILCM growth or its removal has been termed *gill remodelling*. Furthermore, certain gill cell types have been shown to reorganize in the presence or absence of the ILCM. For example, the mitochondrion-rich cells (MRCs; hereafter referred to as *ionocytes*), which are responsible for ion uptake in freshwater (FW) fish, are redistributed to the edges of the ILCM when goldfish are exposed to cold temperatures (Mitrovic et al., 2009; Bradshaw et al., 2012). Redistribution of ionocytes from the gill filament to the lamella as well as their overall proliferation has been reported for several FW species in response to exposure to ion-poor water (Mattheij and Stroband, 1971; Thomas et al., 1988; Perry and Laurent, 1989; Greco et al., 1996; Jonz and Nurse, 2006). Clearly the capacity to reorganize the ionocytes to sustain ionic homeostasis has been conserved in a variety of fish

© 2013 Wiley Periodicals, Inc.

species. The importance of ionocyte redistribution as a compensatory mechanism is illustrated by the fact that, in species such as rainbow trout, the redistribution of ionocytes in ion-poor water (or after treatment with osmoregulatory hormones such as cortisol or growth hormone) occurs despite an associated thickening of the lamellar epithelia, which concurrently limits respiratory gas transfer (Thomas et al., 1988; Bindon et al., 1994; Greco et al., 1996).

To allow ionic uptake, the ionocytes are equipped with a variety of channels, exchangers, and pumps (Perry et al., 2003). As early as 1939 (Krogh, 1939), it was proposed that these ionic uptake mechanisms are under neural control. The gill receives extensive innervation from the facial, glossopharyngeal, and vagus nerves (cranial nerves VII, IX, and X, respectively, also referred to as the *branchial nerves*; Nilsson, 1984, Sundin and Nilsson, 2002). In a study of osmoregulation in the eel *Anguilla anguilla*, Mayer-Gostan and Hirano (1976) showed that denervation of the branchial nerves caused an increase in plasma ion concentrations in fish acclimated to seawater. More recently, Jonz and Nurse (2006) demonstrated that branchial ionocytes (identified on the basis of Na^+/K^+-ATPase [NKA] immunoreactivity) in adult zebrafish are innervated by nerve fibers whose cell bodies are located outside the gill filaments. More recently, Kumai et al. (2012) demonstrated neuronal innervation of the H^+-ATPase-rich (HR) cells of larval zebrafish skin, ionocytes known to be involved in Na^+ uptake and H^+ excretion (Lin et al., 2006; for reviews see Kumai and Perry, 2012; Dymowska et al., 2012) The exact nature of the fibers innervating the ionocytes has not been clearly determined, but there is evidence that they may be adrenergic (Donald, 1989; Kumai et al., 2012).

Despite their presumed role in regulating ionocyte function, nothing is known about whether (or how) ionocyte innervation is preserved during gill remodeling when ionocyte migration or redistribution occurs. Maintaining innervation to branchial ionocytes may be particularly challenging for goldfish owing to the drastic changes in gill morphology that they can experience. This study addresses the question of how gill remodelling in goldfish affects ionocyte turnover and innervation. We hypothesize that, as the ILCM is shed during hypoxia-induced gill remodelling, there will be a loss (or migration) of the pre-existing ionocytes on its outer edges coupled with the formation of new ionocytes. The consequences of ionocyte loss, migration, and de novo differentiation during gill remodelling on the pattern of ionocyte neuronal innervation are unknown. Thus, the aims of this study were 1) to determine and quantify gill ionocyte numbers and innervation in goldfish kept at 7°C (ILCM present) and 25°C (ILCM absent) and 2) to show changes in ionocyte turnover and innervation in goldfish at 7°C undergoing gill remodelling induced by hypoxia with or without normoxic recovery.

MATERIALS AND METHODS
Experimental animals
Small (10–12.7 cm in length) goldfish of both sexes were purchased from a commercial supplier (Aleong's International, Mississauga, Ontario, Canada). Upon arrival, the fish were placed in circular tanks supplied with aerated and dechloraminated water at 18°C. One group of fish was acclimated to 7°C and another was acclimated to 25°C over a 2-week period by either increasing or decreasing the water temperature by ~2°C per day. The fish were held at their temperatures for a minimum of 14 days on a 12:12-hour light–dark photoperiod and were fed commercial food pellets (Martin ProFishent Classic floating pellets; Martin Mills Inc., Elmira, Ontraio, Canada) before experimentation. All experiments were performed at the University of Ottawa Aquatic Care Facilities at either 7°C or 25°C in accordance with University of Ottawa Animal Care Committee Protocol BL-226.

Experimental protocol
Hypoxia and steady-state experiments
Goldfish acclimated to 7°C (average mass 23.0 ± 3.0 g; N = 26) were placed individually into 600-ml opaque boxes supplied with flowing normoxic water (PO_2 ~155 mm Hg). The fish were then exposed to hypoxia (PO_2 10 mm Hg) for 7 days. Hypoxia was achieved by gassing a water equilibration column with N_2 and water; oxygen levels were monitored continuously using an oxygen electrode (Cameron Instruments) connected to a gas meter (Cameron Instruments BGM 200). In some experiments, normoxic water flow was returned for 1–2 weeks. Goldfish kept at 7°C or 25°C under normoxic conditions were used as controls.

Immunohistochemistry
Pre-existing ionocytes were identified by bathing goldfish for 6 hours in 0.5 μmol MitoTracker Red (MitoTracker Red CMXRos; Molecular Probes, Eugene OR). Fish were exposed to this fluorescent mitochondrion-specific dye either prior to hypoxia (for the fish that were not allowed to recover under normoxic conditions) or just before commencing the period of normoxic recovery (for the fish that were allowed to recover from the hypoxic exposure). At the end of the experiments, the fish were killed by anesthetic overdose (benzocaine;

Antibody	Immunogen	Manufacturer, species antibody was raised in, mono- vs. polyclonal	Dilution	Primary antibody used in goldfish and other species	References
α-5	Na^+/K^+-ATPase α subunit	University of Iowa Hybridoma Bank, mouse, monoclonal	1:100	Brown trout (*Salmo trutta*) Atlantic salmon (*Salmo salar*) Killifish (*Fundulus heteroclitus*) Sea bass (*Morone saxatilis*) Goldfish (*Carassius auratus*)	Tipsmark et al. (2002) Marshall et al. (2002) Tipsmark et al. (2004) Bradshaw et al. (2012)
zn-12	HNK-1-like sugar epitope	University of Iowa Hybridoma Bank, mouse, monoclonal	1:100	Zebrafish (*Danio rerio*) Goldfish (*Carassius auratus*)	Trevarrow et al. (1990) Marshall et al. (1990) Jonz and Nurse (2006) Saltys et al. (2006)

ethyl-*P*-amino-benzoate, 2.4×10^{-4} mol liter^{-1}; Sigma, St. Louis, MO), and the first right gill arch from each fish was removed and fixed in 4% paraformaldehyde (PFA) until it was ready for staining. The rakers were removed, and the remaining gill tissue was placed in permeabilizing solution containing 5% Triton X-100 in phosphate-buffered saline (PBST; pH 7.4) overnight. Nerve fibers and the total number of ionocytes were identified using primary antibodies against zebrafish-derived neuron-specific antigen (zn-12; 1:100) and the α-subunit of the Na^+/K^+-ATPase (α-5; 1:100), respectively; these antibodies were obtained from the University of Iowa Hybridoma Bank (http://dshb.biology.uiowa.edu/). Fluorescently conjugated secondary antibodies (Alexa Fluor 488 or Alexa Fluor 594) were used to visualize the nerve fibers and ionocytes. A previous study demonstrated excellent correlation between cells stained with MitoTracker and those stained with the Na^+/K^+-ATPase antibody (Mitrovic et al., 2009). Gills were then placed on concave slides containing Vectashield (Vector, Burlington, Ontario, Canada) mounting medium. The gill tissue was examined using a confocal microscope (Zeiss LSM 510 Meta) with argon (peak output 488 nm) and helium-neon (peak output 543 nm) lasers. A Z-stack was created by taking optical slices (1–3 μm thickness) through the gill tissue and using LSM Image Browser (Carl Zeiss Microscopy, Jena, Germany) and Image J software (http://rsbweb.nih.gov.proxy.bib.uottawa.ca/ij/index.html) to generate a three-dimensional composite image. Photoshop CS3 (Adobe Systems, San Jose, CA) software was used to create the final composite images and to correct for contrast and brightness.

Antibody characterization

The primary antibodies used in this study are summarized in Table 1. Previous studies have demonstrated that the α-5 antibody recognizes a single band at the expected size of ~115 kD on Western blots prepared from gill tissue in numerous fish species (e.g., Wilson et al., 2000), including goldfish (V. Tzaneva, unpublished data) . The α-5 antibody was developed by D.M. Fambrough at Johns Hopkins University. It is directed against the chicken Na^+/K^+-ATPase $α_1$ subunit and binds to all isoforms across species. Its specificity for use in immunohistochemistry (IHC) has long been established for all teleost fish examined, including trout, salmon, killifish, and sea bass (Marshall et al., 2002; Tipsmark et al., 2002, 2004). Recently, the α-5 antibody was used to identify ionocytes in the gills of goldfish acclimated to 7°C (Bradshaw et al., 2012).

The zn-12 antibody was developed against the zebrafish HNK-1 (human natural killer-1)-like sugar epitope by B. Trevarrow at the University of Oregon. Metcalfe et al. (1990) demonstrated the specificity of the antibody to HNK-1-like sugar epitope in zebrafish embryos by showing that both the zn-12 and HNK-1 antibodies produce the same pattern of bands on a Western blot. In this study, the zn-12 antibody generated multiple bands at ~90, 70, and 60 kD on Western blots of goldfish gill tissue. This immunolabeling pattern is similar to that obtained for zebrafish by Metcalfe et al. (1990). In addition, the zn-12 antibody was used previously to label neurons in the gills of both zebrafish and goldfish (Jonz and Nurse, 2006; Saltys et al., 2006).

Ionocyte quantification

For each fish (gill arch), six gill filaments were selected randomly for imaging, producing six images per fish. Ionocytes and associated innervation were quantified in the upper, middle, and lower regions of each filament by scrolling through the sections of the Z stack and counting the number of ionocytes present and whether or not they were innervated. The area of each region of

the filament was determined by selecting three lamellae and outlining them using the rectangle tool in the LSM Image Browser, which automatically calculated the area in square millimeters. Cells were classified as innervated only when a nerve clearly touched the cell surface. The lamellar and filament ionocytes of six composite images representing different filaments were counted and averaged to generate a value of ionocyte/mm^2 or as a percentage of the total ionocyte population per fish.

Statistical analysis

Data are presented as mean $\pm$ SEM. Student's *t*-test, one-way analysis of variance (ANOVA), or one-way ANOVA on ranks (when assumptions for parametric analysis were not met) were used to test for significant differences between means. Holm-Sidak or Dunn's post hoc tests were used when significant differences were revealed by ANOVA. The fiducial limit of significance was 0.05 for all analyses. SigmaPlot v. 11.0 (SPSS Inc., Cary, NC) was used to perform all the statistical analyses.

RESULTS

Goldfish during steady-state normoxia

Figure 1 summarizes the number of total ionocytes/mm^2 of filament (Fig. 1A), the percentage of innervated ionocytes (Fig. 1B), and the total number of innervated ionocytes/mm^2 (Fig. 1C) in normoxic goldfish kept at 7°C or 25°C. Cold-acclimated goldfish (7°C) exhibited a significantly greater number of ionocytes/mm^2 of filament (951.2 $\pm$ 94.3) than their warm-acclimated (25°C) conspecifics (363.1 $\pm$ 49.6; Fig. 1A; $P <$ 0.001). The total number of innervated ionocytes/mm^2 in cold acclimated goldfish was 788.1 $\pm$ 73.7, which is considerably higher than the number of innervated ionocytes/mm^2 in warm-acclimated goldfish (318.2 $\pm$ 41.7; *t*-test, $P <$ 0.001). Although warm-acclimated goldfish had fewer total ionocytes per area and innervated ionocytes per area, the percentage of innervated ionocytes (87.8% $\pm$ 1.3%) was significantly higher than in the cold-acclimated goldfish (83.1% $\pm$ 1.0%).

The gill morphology of 7°C and 25°C goldfish is depicted in Figures 2 and 3, respectively. The extent of gill remodelling was not quantified in this study because it has been thoroughly investigated in previous studies (see, e.g., Mitrovic et al., 2009; Tzaneva et al., 2011). Figure 2 shows the distribution and innervation of ionocytes on a 7°C goldfish gill filament with its ILCM filling the interlamellar channels. The ionocytes of 7°C goldfish were distributed predominantly, though not exclusively, toward the outer edges of the ILCM (Fig. 2A),
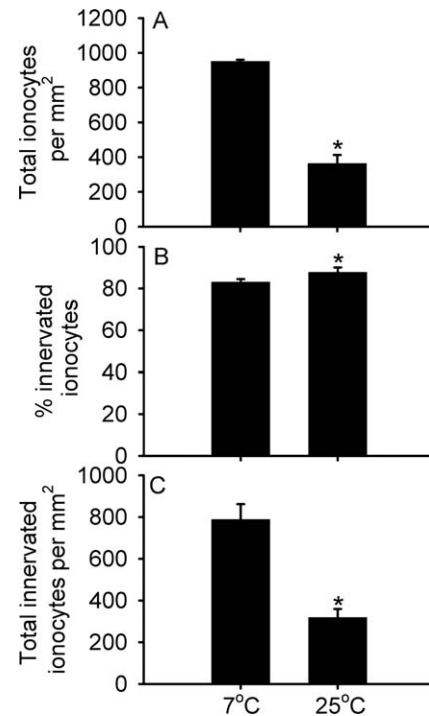
Figure 1. Mean data representing the number of total ionocytes/mm^2 (**A**), the percentage innervated ionocytes from the total population of ionocytess (**B**), and the total number of innervated ionocyess/mm^2 (**C**) in normoxic goldfish kept at either 7°C or 25°C; N = 6 for all. Data are mean $\pm$ SEM. Asterisks represent statistically significant changes from the 7°C state (*t*-test, $P < 0.05$).

with nerves typically surrounding the cell (Fig. 2B,C). In contrast, 25°C goldfish lacked an ILCM, and the ionocytes were located largely at the base of the lamella or in the interlamellar region (Fig. 3A). Innervated ionocytes were clearly visible on the gills of warm-acclimated goldfish (Fig. 3B,C).

### Hypoxia exposure with or without 1–2 weeks of normoxic recovery
Qualitative analysis

Figures 4–6 show the distribution and innervation of pre-existing and newly formed ionocytes in hypoxia-exposed fish with and without 1–2 weeks of normoxic recovery. After hypoxia (Fig. 4), the ILCM was retracted, and the gill morphology resembled that of a 25°C goldfish, the ionocytes being localized to the base of the lamella in the interlamellar region (Fig. 4E). Figure 4C clearly shows a pre-existing (i.e., present prior to beginning the hypoxia exposure) innervated ionocyte (shown in yellow) and a new ionocyte (shown in green). Figure 4A shows evidence of a newly formed ionocyte, and Figure 4B illustrates only pre-existing ionocytes. An ortho-view of Figure 4C is shown in Figure 4D to confirm further that the ionocyte is indeed innervated. The
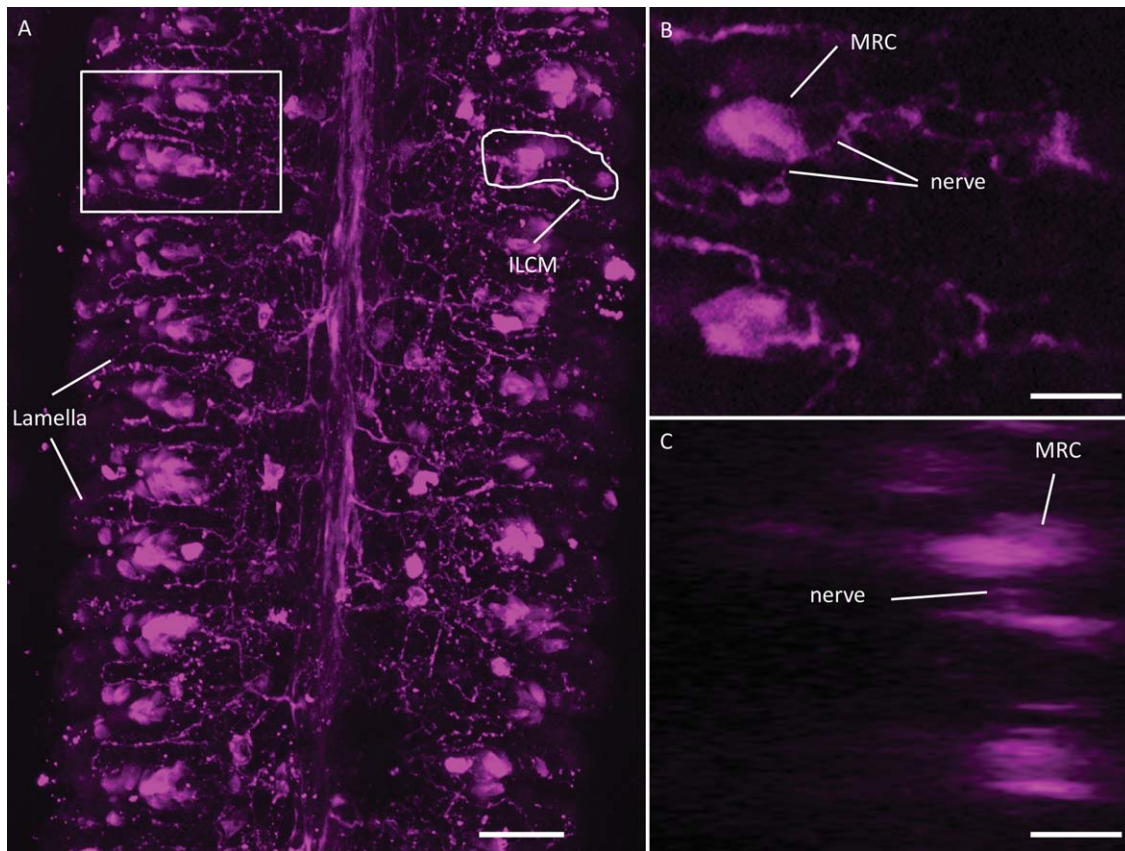
Figure 2. Micrographs representing the distribution of ionocytes and their associated innervation on the gills of steady-state, normoxic 7°C goldfish with the interlamellar cell mass present (ILCM). **A:** The majority of ionocytes stained with the α-5 antibody (magenta) remained exposed to the external environment in the presence of the ILCM. **B:** Magnified view of the zn-12-positive staining (magenta) of nerves associated with ionocytes. **C:** Image from B rotated 90° along the horizontal axis to demonstrate further an innervated MRC. Scale bars = 50 μm in A; 25 μm in B,C.
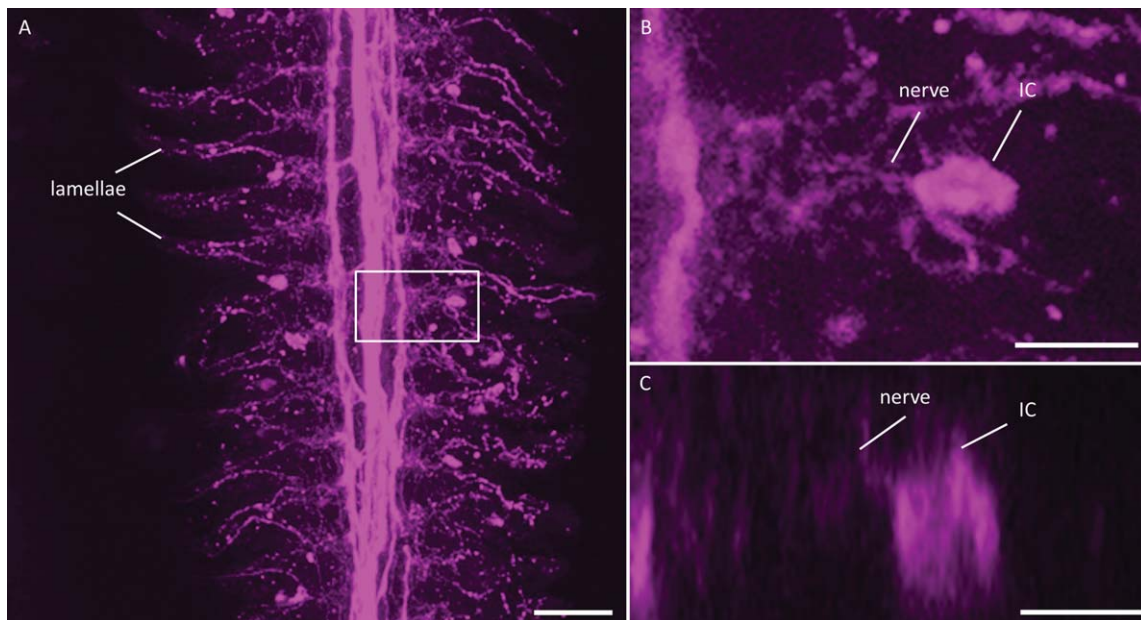
Figure 3. Micrographs representing the distribution of ionocytes and their associated innervation on the gills of steady-state, normoxic 25°C goldfish with the interlamellar cell mass (ILCM) absent. **A:** The majority of ionocytes stained with α-5 antibody (magenta) remained exposed to the external environment and were found at the base of the lamellae in the interlamellar region. **B:** Magnified view of the zn-12-positive staining (magenta) of nerves associated with MRCs. **C:** Image from B rotated 90° along the horizontal axis to demonstrate further an innervated MRC. Scale bars = 50 μm in A; 25 μm in B,C.
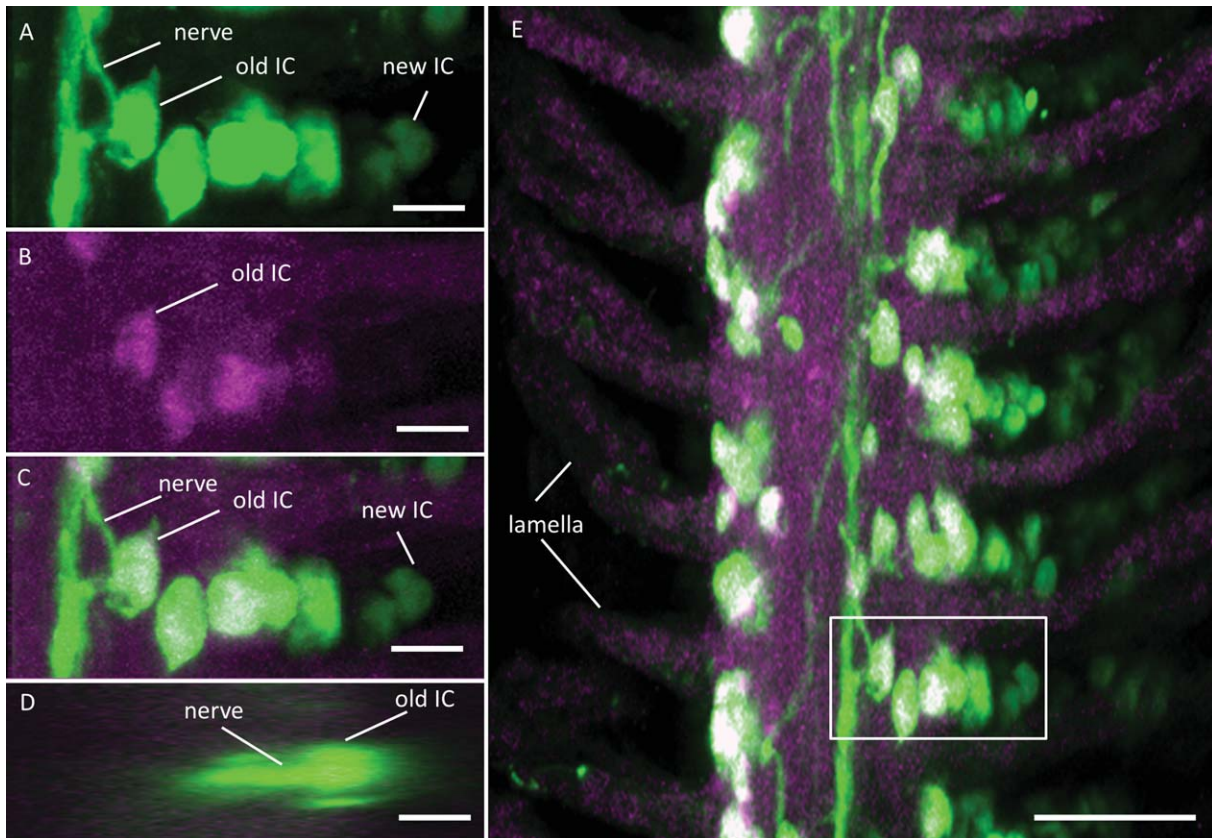
Figure 4. Light micrographs depicting the distribution of ionocytes (IC) and their associated innervation on the gills of 7°C goldfish exposed to hypoxia without normoxic recovery. Goldfish were bathed in MitoTracker Red before hypoxia exposure and then stained with α-5 antibody 7 days after the hypoxia exposure so that pre-existing ionocytes appeared red (converted to magenta) and newly formed ionocytes appeared green. **A:** Magnified view of α-5-positive staining of both pre-existing and new ionocytes with any associated innervation (zn-12-positive staining in green). **B:** Pre-existing ioncytes stained with MitoTracker Red (magenta). **C:** Overlap between A and B to distinguish clearly a pre-existing ionocyte (white) from a newly formed cell (green) and any zn-12-positive nerves (green) associated with the cells. **D:** Image C rotated 90° along the horizontal axis, demonstrating the innervation of a pre-existing ionocyte. **E:** Distribution of all ionocytes along the gill filament with most of the cells found along the base of the interlamellar region. Scale bars = 25 μm in A–D; 50 μm in E.

gill morphology of goldfish exposed to 1 week of hypoxia and 1 week of recovery is shown in Figure 5. The interlamellar space was not fully occupied by the ILCM, and the ionocytes were situated at the base of the lamella as well as at the edges of the ILCM (Fig. 5D). Pre-existing ionocytes were labeled with both Mito-Tracker Red (Fig. 5A) and the α-5 antibody (Fig. 5B) to distinguish them from newly formed ionocytes, which were marked only with the α-5 antibody and thus appeared green (Fig. 5C). The innervation of a pre-existing ionocyte can be seen in Figure 5C and was further demonstrated by rotating the 3D image by 90° to obtain a cross-sectional view of the filament (Fig. 5D). The ILCM did not fully reappear after 2 weeks of normoxic exposure (Fig. 6D). The ionocytes (both pre-exisiting and new), however, had mostly redistributed to the edge of the ILCM, with few remaining at the base

of the lamellae (Fig. 6A,B,D). Figure 6C,E shows the innervation of pre-existing ionocytes in goldfish exposed to 1 week of hypoxia with 2 weeks of normoxic recovery.

Quantitative analysis

Three groups of 7°C goldfish were exposed to hypoxia, and gill tissue was collected after hypoxia (without normoxic recovery), 1 week after normoxic recovery, or after 2 weeks of normoxic recovery. The numbers of total, pre-existing, and new ionocytes and their associated innervation were quantified for each group. There were no significant differences among groups for the numbers of new, pre-existing, or total ionocytes/mm^2 (Fig. 7). In goldfish that did not experience normoxic recovery, the number of pre-existing ionocytes/mm^2 was 555.6 ± 38.1, which was significantly higher than
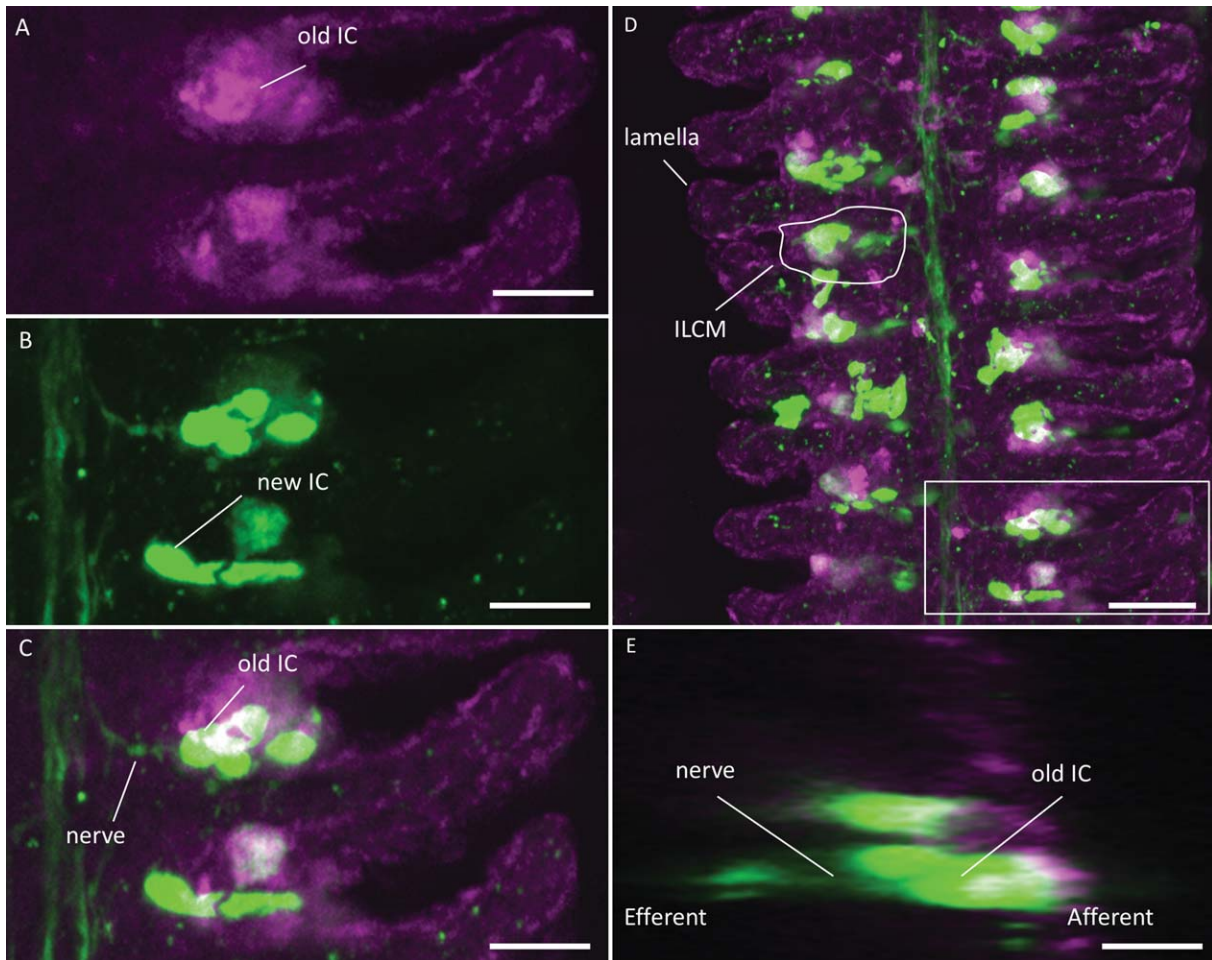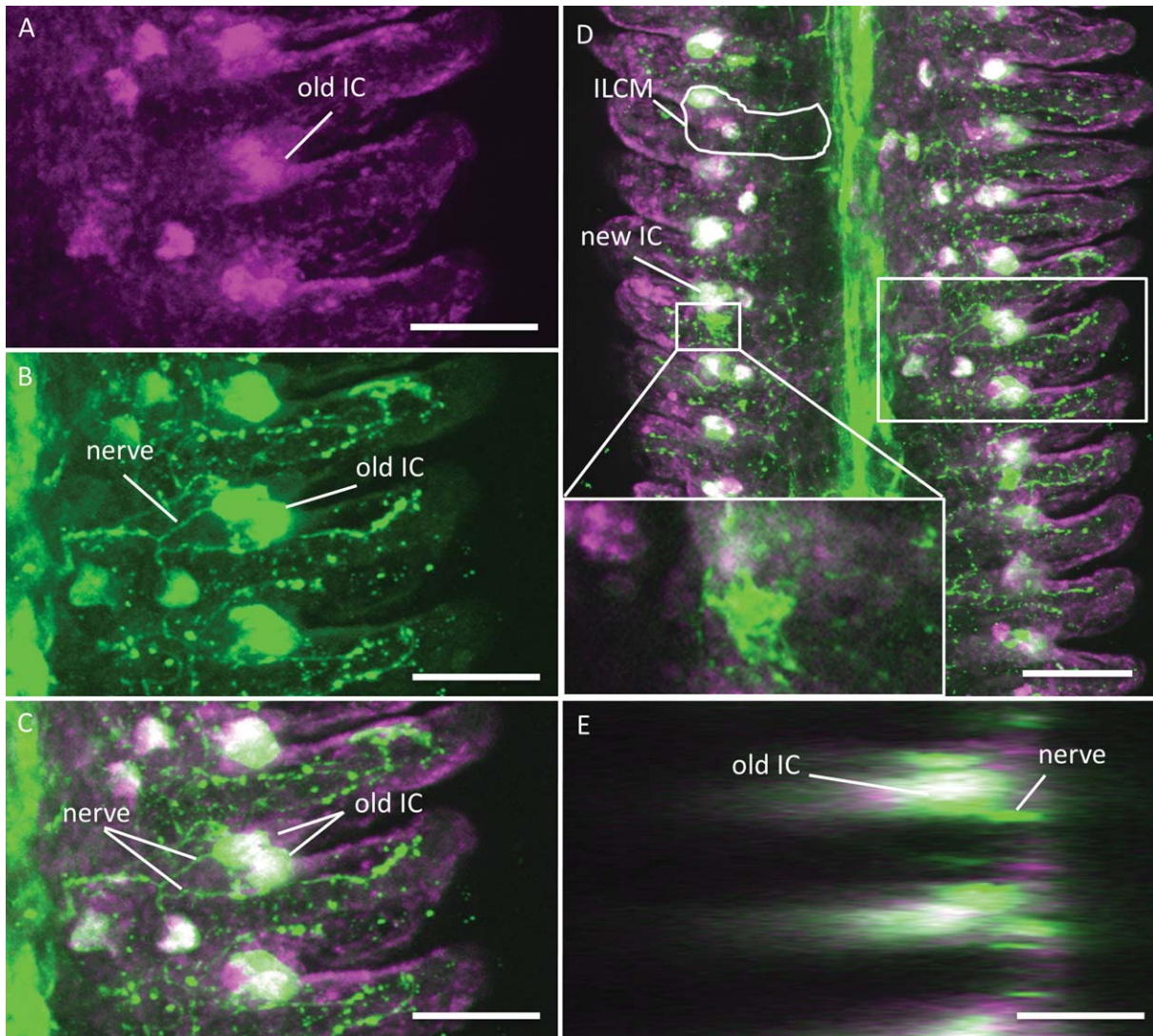
Figure 5. Light micrographs depicting the distribution of ionocytes (IC) and their associated innervation on the gills of 7°C goldfish exposed to hypoxia with 1 week of normoxic recovery. Goldfish were bathed in MitoTracker Red immediately after hypoxia exposure and then stained with α-5 antibody 1 week after the normoxic recovery so that pre-existing ionocytes appeared red (converted to magenta) and newly formed cells appeared green. **A:** Magnified view of α-5-positive staining of both pre-existing and new ionocytes with any associated innervation (zn-12-positive staining in green). **B:** Pre-existing ionocytes stained with MitoTracker Red (magenta). **C:** Overlap between A and B to distinguish clearly a pre-existing ionocyte (white) from a newly formed cell (green) and any zn-12-positive nerves associated (green) with the cells. **D:** Distribution of all ionocytes along the gill filament with most of the cells found along the edge of the interlamellar cell mass (ILCM), with some still persisting at the base of the interlamellar region. **E:** Image C rotated 90° along the horizontal axis, further demonstrating the innervation of a pre-existing ionocyte. Scale bars = 25 μm in A–C,E; 50 μm in D.

the number of new ionocytes, 226.7 ± 15.1 ionocytes/mm^2, for a total of 782.3 ± 51.2 ionocytes/mm^2 (Fig. 7; ANOVA, $P < 0.001$).

In goldfish exposed to 1 week of normoxia recovery, the total number of ionocytes/mm^2 (938.1 ± 137.4) was made up of roughly equivalent numbers of new (331.0 ± 63.7) and pre-existing (607.1 ± 100.2) ionocytes (Fig. 7). Although there was a trend toward an increasing proportion of pre-existing ionocytes (993.4 ± 291.1) to the total ionocyte population ($1,384.6 \pm 380.1$) in fish experiencing 2 weeks of normoxic recovery, the large variability of the data set prevented statistical confirmation.

Figure 8 illustrates the differences in the number of innervated ionocytes within and between treatment groups. One-way ANOVA did not reveal any statistically significant differences between treatment groups for numbers of total, pre-existing, or new innervated ionocytes. Goldfish that had not experienced normoxic recovery possessed predominantly pre-existing innervated ionocytes, 449.2 ± 127.2/mm^2, compared with only 190.3 ± 45.8 new innervated ionocytes/mm^2. There were no significant differences between numbers of pre-existing and new innervated ionocytes for goldfish that had experienced only hypoxia. The total number of innervated ionocytes/mm^2 for goldfish without

Figure 6. Light micrographs representing the distribution of ionocytes (IC) and their associated innervation on the gills of 7°C goldfish exposed to hypoxia with 2 weeks normoxic recovery. Goldfish were bathed in MitoTracker Red immediately after hypoxia exposure and then stained with α-5 antibody 2 weeks after the normoxic recovery so that pre-existing ionocytes appeared red (converted to magenta) and newly formed cells appeared green. **A:** Magnified view of α-5-positive staining of both pre-existing and new ionocytes with any associated innervation (zn-12-positive staining in green). **B:** Pre-existing ionocytes stained with MitoTracker Red (magenta). **C:** Overlap between A and B to distinguish clearly a pre-existing ioncyte (white) from a newly formed cell (green) and any zn-12-positive nerves (green) associated with the cells. **D:** Distribution of all ionocytes along the gill filament, with most of them found along the edge of the interlamellar cell mass (ILCM). **Inset** shows a magnified view of a newly formed ionocyte. **E:** Image C rotated 90° along the horizontal axis, further demonstrating the innervation of a pre-existing ioncyte. Scale bars = 25 μm in A–C,E; 50 μm in D.

recovery was 616.4 $\pm$ 40.8, which is only significantly higher than the number of new innervated ionocytes/mm^2 (151.7 $\pm$ 10.9; ANOVA, $P < 0.001$). Similarly, the total population of innervated ionocytes of goldfish exposed to 1 week of normoxic recovery (357.9 $\pm$ 79.8/mm^2) consisted primarily of pre-existing innervated cells (242.2 $\pm$ 61.4/mm^2). After 2 weeks of normoxia recovery, there was no statistical differences between the numbers of total (639.0 $\pm$ 168.9/mm^2),

pre-existing (449.2 $\pm$ 127.2/mm^2), and new (190.3 $\pm$ 45.8/mm^2) innervated ionocytes, although there was a trend toward greater numbers of pre-existing ionocytes (ANOVA, $P = 0.063$).

In keeping with the trends depicted in Figures 7 and 8, pre-existing ionocytes exhibited a significantly higher percentage of innervation than newly formed ionocytes (Fig. 9). Cold-acclimated goldfish exposed to hypoxia without normoxic recovery had 59.5% $\pm$ 1.8% of their
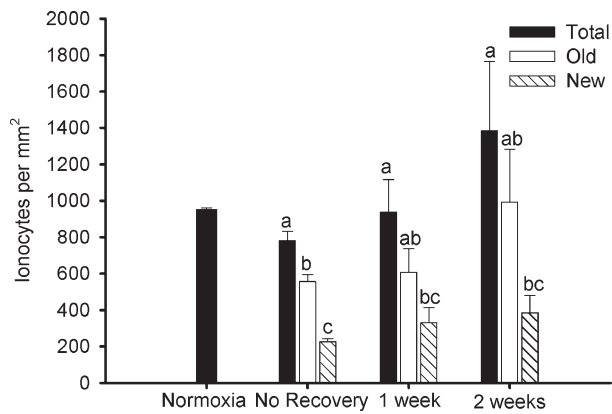
Figure 7. Effects of hypoxia and either 1 or 2 weeks of normoxic recovery on the total (solid bar), pre-existing (open bar),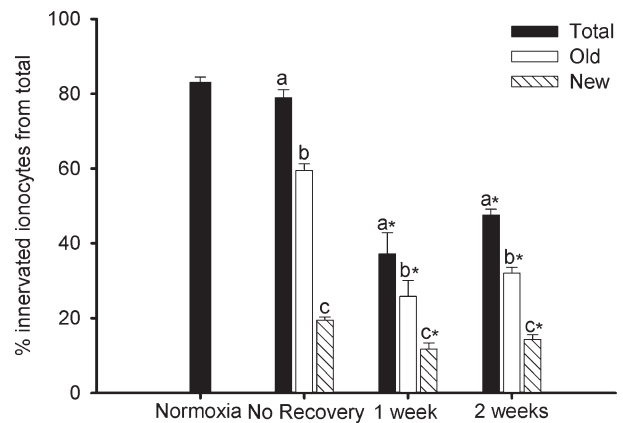 and new (hatched bar) numbers of ionocytes/mm^2 in 7°C goldfish. There were no statistically significant differences between treatment groups. Letters represent significant differences within treatments among total, pre-existing, and new ionocytes (one way ANOVA, $P < 0.05$). N = 6 for goldfish only exposed to normoxia (normoxia); N = 5 for goldfish exposed to hypoxia without normoxic recovery (no recovery) and with 1 week of normoxia recovery (1 week); N = 4 for goldfish exposed to hypoxia with 2 weeks of normoxic recovery (2 weeks). Data are represented as mean ± SEM.
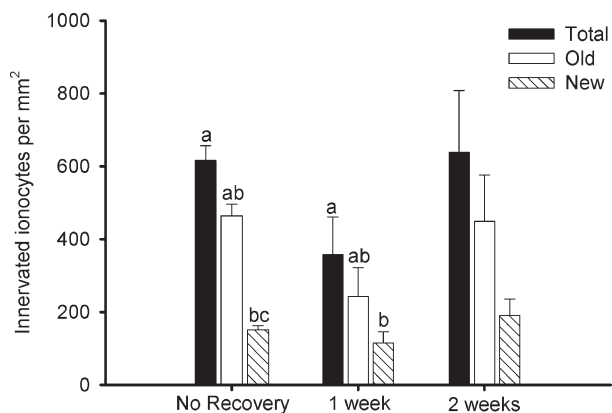
Figure 8. Effects of hypoxia on the number of total (solid bar), pre-existing (open bar), and new (hatched bar) innervated ionocytes/mm^2 in 7°C goldfish without normoxic recovery (no recovery; N = 5), with 1 week of normoxic recovery (1 week; N = 5), or with 2 weeks of normoxic recovery (2 weeks; N = 4). No statistically significant differences were detected among groups for the total, pre-existing, or new innervated ionocytes. There was no significant difference among the number of total, pre-existing, and new innervated ionocytes for the 2 week group. Letters represent statistically significant differences within a treatment. Data are presented as mean ± SEM.

pre-existing ionocytes innervated compared with only 19.4% ± 0.8% innervation of newly formed ionocytes (ANOVA on ranks, $P < 0.001$). The percentages of innervation of total, pre-existing, and new ionocytes

Figure 9. Effects of hypoxia on the percentage innervation of total (solid bar), pre-existing (open bar), and new (hatched bar) ionocytes in 7°C goldfish kept in normoxic water (normoxia; N = 6) or exposed to hypoxia without normoxic recovery (no recovery; N = 5), with 1 week of normoxic recovery (1 week; N = 5), and with 2 weeks of normoxic recovery (2 weeks; N = 4). Letters represent significant differences within treatment groups. Asterisks represent diffgerences among groups for the percentage innervation of total, pre-existing, or new ionocytes. Data are represented as mean ± SEM (one-way ANOVA, $P < 0.05$).

were all significantly different from each other in goldfish exposed to 1 week of normoxic recovery (ANOVA, $P < 0.001$). After 1 week of recovery in normoxic water, the total percentage of innervated ionocytes was 37.2% ± 4.3%, owing to 25.8% ± 4.3% innervation of pre-existing ionocytes and 11.7% ± 1.6% innervation of newly formed ionocytes. After 2 weeks of recovery, the total percentage of innervated ionocytes increased significantly to 47.5% ± 1.6% (ANOVA, $P < 0.001$) but was still lower than in goldfish that had not been allowed to recover (ANOVA, $P < 0.001$). The percentage innervation of pre-existing ionocytes was also higher after 2 weeks of normoxic exposure (32.0% ± 1.5%) compared with the 1-week recovery group; however, it remained significantly lower than in goldfish that had not experienced normoxia after hypoxic exposure (ANOVA, $P < 0.001$). Surprisingly, the percentage innervation of newly formed ionocytes significantly decreased from 19.5% ± 0.8% in hypoxia-exposed goldfish without recovery to 11.7% ± 1.6% and 14.3% ± 1.3% in 1- and 2-week normoxic recovery groups, respectively (ANOVA, $P < 0.002$), without a significant difference between the percentages of innervation of new ionocytes in 1- and 2-week normoxic recovery groups. In the 2-week normoxic recovery group, the differences in percentage innervation among the total, pre-existing, and new ionocytes were all significantly different from each other (ANOVA, $P < 0.001$).

DISCUSSION

The overall aim of this study was to assess the fate of ionocytes and their associated neuronal innervation in goldfish during hypoxia-induced gill remodelling and subsequent recovery in normoxic water. Specifically, we sought to determine whether the migration of pre-existing ionocytes with the loss and regrowth of the ILCM and the formation of new ionocytes would alter the nature of their neuronal innervation. The major findings were that 1) fish acclimated to 25°C possessed significantly fewer numbers of ionocytes, but a greater percentage of them were innervated in comparison with the fish acclimated to 7°C; 2) 7°C goldfish exposed to hypoxia without normoxic recovery or after 1–2 weeks of recovery had fewer new ionocytes; 3) pre-existing ionocytes showed a significantly higher percentage of innervation than newly formed ionocytes; and 4) overall innervation of ionocytes decreased in goldfish exposed to 1–2 weeks of normoxic recovery.

Distribution of ionocytes

In agreement with previous studies (Mitrovic and Perry, 2009; Mitrovic et al., 2009; Bradshaw et al., 2012), the branchial ionocytes in goldfish acclimated to 7°C were localized predominantly to the edges of the ILCM, with relatively few cells found within the ILCM itself. This spatial distribution differed from that observed in the 25°C-acclimated conspecifics, in which the ionocytes were located primarily in the interlamellar regions near the filament. In 7°C goldfish, hypoxia exposure caused the redistribution of ionocytes from the distal edges of the ILCM to the interlamellar regions. Subsequent prolonged exposure to normoxia caused their relocation back to the edge of the ILCM. The redistribution of ionocytes toward the outer edges of the ILCM likely serves to maintain maximal exposure of the ionocytes to the external environment and thus may be advantageous for sustaining the ion transport capacity of the gill.

Experiments conducted on 7°C hypoxic goldfish, however, revealed a decrease in unidirectional Na^+ fluxes after hypoxia exposure (Bradshaw et al., 2012). Similar results were obtained for the scaleless carp (*Gymnocypris przewalskii*), which also experiences gill remodelling (Matey et al., 2008). Matey and colleagues (2008) reported that hypoxia exposure of 11–15°C-acclimated scaleless carp was associated with a 10–15% decrease in plasma [Na^+]. These authors also reported that plasma [Na^+] returned to normal levels as the fish were re-exposed to normoxia and the ILCM began to reoccupy the interlamellar space.

Unlike the case in a previous study (Mitrovic et al., 2009) that reported a decrease in the number of iono-cytes, the total number of ionocytes did not change significantly after hypoxia exposure, and the majority of ionocytes remained exposed during normoxic recovery. These results suggest that conserving pre-existing ionocytes coupled with the differentiation of new ionocytes during hypoxia may be a mechanism to maintain ion transport capacity in expectation of a normoxic recovery and subsequent return to the previous metabolic state. Thus, it is possible that the morphological adjustments of the gill during hypoxia in 7°C goldfish (shedding the ILCM) might initially favor O_2 uptake by increasing the functional surface area and decreasing the water-to-blood diffusion distance. Additionally, ion uptake is reduced to conserve energy, but the ionocytes remain exposed to the external environment, ready to resume their activity once normoxia has been restored.

Ionocyte turnover (renewal) in the gill epithelia in fish acclimated to 7°C

The majority of the ionocytes present at the end of each treatment (hypoxia only, 1 week recovery, and 2 week recovery) were pre-existing ionocytes, with relatively few new cells. Certainly, retaining pre-existing ionocytes is advantageous to lower the energetic costs that would otherwise have to be invested into cell differentiation after hypoxia-induced gill remodelling (Sollid et al., 2003, 2005; Bradshaw et al., 2012). The total number of ionocytes did not change significantly in hypoxia-exposed fish compared with their normoxic conspecifics. There was a trend toward a decrease in the number of pre-existing ionocytes compared with the total number of ionocytes in all 7°C groups that had been exposed to hypoxia. This suggests that some of the cells have died or have been shed with the ILCM during the hypoxia exposure and that new ionocytes were differentiated to maintain the total number of cells available for ion transport. Previous studies have shown that environmental (changes in salinity) and hormonal (e.g., growth hormone, prolactin) factors can stimulate the differentiation of new ionocytes in the gills of teleost fish (Pisam et al., 1993; Prunet et al., 1994; Tsai and Hwang, 1998). To our knowledge, this is the first study to demonstrate that changes in ambient O_2 can also trigger the differentiation of new ionocytes in the gills of goldfish (Figs. 7–9).

Ionocyte innervation and possible mechanisms of ion regulation

This is the first study to our knowledge to investigate reversible gill remodelling and ionocyte distribution *and* their associated innervation. The results revealed that the percentage of innervated ionocytes in 7°C fish exposed to hypoxia was unchanged immediately after hypoxic exposure but then decreased with prolonged

normoxic exposure. We propose that the nerves associated with the ionocytes migrate along with the ionocytes as the ILCM retracts during hypoxia. The fact that the majority of cells (>75%) remained innervated after hypoxia suggests that innervation may be a prerequisite for ionocytes to remain fully functional. A previous study (Pequignot and Gas, 1971) showed that gill denervation reduces the number of ionocytes, further supporting the view that innervation is necessary for the survival of differentiated, functional ionocytes.

Despite maintaining a constant total number of ionocytes during hypoxic exposure and subsequent normoxic recovery, the percentage innervation of these cells decreased throughout the 2-week period of recovery (Fig. 6). We suggest that the ILCM proliferation and subsequent redistribution of the ionocytes to the edge of the ILCM, during the normoxic recovery, may occur more quickly than the regeneration of neural connections between ionocytes and nerves. Previous studies show that the complete regrowth of the ILCM can occur within 2 weeks of normoxic recovery (Sollid et al., 2005; Mitrovic et al., 2009). Furthermore, nerve regeneration in fish, specifically regeneration of the optic nerve in goldfish, can take up to 40 days to re-establish connections with the target cells (Matsukawa et al., 2004). Thus, the possible slow regeneration of branchial nerves coupled with a relatively quick ILCM regrowth during normoxia may account for the decrease in ionocyte innervation during the 1–2-week recovery period that we report in this study. Furthermore, the presence of the ILCM reduces ion efflux across the goldfish gill, which may be sufficient to maintain ion homeostasis during the time in which the ionocytes are re-establishing their innervation (Bradshaw et al., 2012).

The movement of ions across the gill epithelium may be dependent on neurotransmitters released from presynaptic terminals influencing ion channels/transporters within the ionocytes. Marshall et al. (1998) reported that stimulating α-adrenoreceptors resulted in a decrease of Cl– excretion in isolated, nerve-intact opercular epithelium preparations of seawater-acclimated killifish (*Fundulus heteroclitus*). These findings, among others, led to a model of inhibition of salt excretion in seawater-acclimated fish initiated by a sympathetic reflex and culminating with the activation of α-adrenoreceptors presumably localized to ionocytes (Degnan et al., 1977; Marshall and Bern, 1980; Marshall et al., 1980). A similar mechanism of adrenergic inhibition of Cl^- influx in FW rainbow trout (*Oncorhynchus mykiss*) was proposed by Perry et al. (1984). Recently, Kumai et al. (2012) reported that translational gene knockdown β_1- and β_{2A}-adrenergic receptors in zebrafish larvae led to significant decreases in Na^+ uptake during exposure to acidic water. Nonadrenergic neuropeptides also have been suggested to play a role in ion transport across the gill epithelium. Neuronal nitric oxide synthase (nNOS or NOS1) has been localized in the branchial nerves of the Atlantic cod (*Gadus morhua*) and "neuroendocrine cells" in the gills of catfish *Heteropneustes fossilis* (Gibbins et al., 1995; Zaccone et al., 2003; for review see Evans, 2002; Zaccone et al., 2006).

CONCLUSIONS

Although hypoxia-induced gill remodelling did not affect the total number of branchial ionocytes, their percentage of innervation decreased significantly over a 2-week period of recovery in normoxic water. To understand more fully the role of ionocyte neuronal innervation in goldfish, it will be important to identify the specific types of fibers that innervate these cells. Furthermore, pharmacological studies involving exposure of the fish to receptor agonists and antagonists will help to elucidate the involvement of the nervous system in the regulation of ion transport across the fish gill.

CONFLICT OF INTEREST STATEMENT

To our knowledge there is no known or potential conflict of interest, including any financial, personal, or other relationships with other people or organizations, within 3 years of beginning the submitted work that could inappropriately influence, or be perceived to influence, this work.

ROLE OF AUTHORS

All authors had full access to all the data in the study and take responsibility for the integrity of the data and the accuracy of the data analysis. Study concept and design: SFP. Acquisition of data: CV, JT, VT. Analysis and interpretation of data: VT, SFP. Drafting of the manuscript: VT. Critical revision of the manuscript for important intellectual content: SFP. Statistical analysis: VT. Obtained funding: SFP. Administrative, technical, and material support: VT, SFP. Study supervision: VT, SFP.

LITERATURE CITED

Bindon S, Gilmour K, Fenwick J, Perry S. 1994. The effects of branchial chloride cell proliferation on respiratory function in the rainbow trout, *Oncorhynchus mykiss*. J Exp Biol 197:47–63.

Bradshaw JC, Kumai Y, Perry SF. 2012. The effects of gill remodeling on transepithelial sodium fluxes and the distribution of presumptive sodium-transporting ionocytes in

goldfish (*Carassius auratus*). J Comp Physiol B 182:351–366.

Chang IC, Lee TH, Yang CH, Wei YY, Chou FI, Hwang PP. 2001. Morphology and function of gill mitochondria-rich cells in fish acclimated to different environments. Physiol Biochem Zool 74:111–119.

Degnan KJ, Karnaky KJ Jr, Zadunaisky JA. 1977. Active chloride transport in the in vitro opercular skin of a teleost (*Fundulus heteroclitus*), a gill-like epithelium rich in chloride cells. J Physiol 271:155–191.

Donald JA. 1989. Adrenaline and branchial nerve stimulation inhibit Ca^{2+} influx into the gills of rainbow trout, *Salmo gairdneri*. J Exp Biol 141:441.

Dymowska AK, Hwang PP, Goss GG. 2012. Structure and function of ionocytes in the freshwater fish gill. Respir Physiol Neurobiol 184:282–292.

Evans DH. 2002. Cell signaling and ion transport across the fish gill epithelium. J Exp Zool 293:336–347.

Fu SJ, Brauner CJ, Cao ZD, Richards JG, Peng JL, Dhillon R, Wang YX. 2011. The effect of acclimation to hypoxia and sustained exercise on subsequent hypoxia tolerance and swimming performance in goldfish (carassius auratus). J Exp Biol 214(Pt 12):2080–2088.

Gibbins IL, Olsson C, Holmgren S. 1995. Distribution of neurons reactive for NADPH-diaphorase in the branchial nerves of a teleost fish, *Gadus morhua*. Neurosci Lett 193:113–116.

Greco AM, Fenwick JC, Perry SF. 1996. The effects of softwater acclimation on gill structure in the rainbow trout oncorhynchus mykiss. Cell Tissue Res 285:75–82.

Jonz MG, Nurse CA. 2006. Epithelial mitochondria-rich cells and associated innervation in adult and developing zebrafish. J Comp Neurol 497:817–832.

Jonz MG, Nurse CA. 2008. New developments on gill innervation: insights from a model vertebrate. J Exp Biol 211:2371–2378.

Krogh A. 1939. The active uptake of ions into cells and organisms. Proc Natl Acad Sci U S A 25:275–277.

Kumai Y, Perry SF. 2012. Mechanisms and regulation of na(+) uptake by freshwater fish. Respir Physiol Neurobiol 184:249–256.

Kumai Y, Ward MA, Perry SF. 2012. *β*-Adrenergic regulation of Na^+ uptake by larval zebrafish *Danio rerio* in acidic and ion-poor environments. Am J Physiol Regul Integr Comp Physiol 303:R1031–R1041.

Lin LY, Horng JL, Kunkel JG, Hwang PP. 2006. Proton pump-rich cell secretes acid in skin of zebrafish larvae. Am J Physiol Cell Physiol 290:C371–C378.

Marshall WS, Bern HA. 1980. Ion transport across the isolated skin of the teleost *Gillichthys mirabilis*. In: Lahlou B, editor. Epithelial transport in the lower vertebrates. New York: Cambridge University Press. p. 337–350.

Marshall WS, Duquesnay RM, Gillis JM, Bryson SE, Liedtke CM. 1998. Neural modulation of salt secretion in teleost opercular epithelium by 2-adrenergic receptors and inositol 1,4,5-trisphosphate. J Exp Biol 201:1959–1965.

Marshall WS, Lynch EM, Cozzi RRF. 2002. Redistribution of immunofluorescence of CFTR anion channel and NKCC cotransporter in chloride cells during adaptation of the killifish *Fundulus heteroclitus* to sea water. J Exp Biol 205:1265–1273.

Matey V, Richards JG, Wang Y, Wood CM, Rogers J, Davies R, Murray BW, Chen XQ, Du J, Brauner CJ. 2008. The effect of hypoxia on gill morphology and ionoregulatory status in the Lake Qinghai scaleless carp, *Gymnocypris przewalskii*. J Exp Biol 211:1063–1074.

Matsukawa T, Arai K, Koriyama Y, Liu Z, Kato S. 2004. Axonal regeneration of fish optic nerve after injury. Biol Pharm Bull 27:445–451.

Mattheij JA, Stroband HW. 1971. The effects of osmotic experiments and prolactin on the mucous cells in the skin and the ionocytes in the gills of the teleost cichlasoma biocellatum. Z Zellforsch Mikrosk Anat 121:93–101.

Mayer-Gostan N, Hirano T. 1976. The effects of transecting the IXth and Xth cranial nerves on hydromineral balance in the eel *Anguilla anguilla*. J Exp Biol 64:461–475.

Metcalfe WK, Myers PZ, Trevarrow B, Bass MB, Kimmel CB. 1990. Primary neurons that express the L2/HNK-1 carbohydrate in the zebrafish. Development 110:491–504.

Mitrovic D, Dymowska A, Nilsson GE, Perry SF. 2009. Physiological consequences of gill remodeling in goldfish (carassius auratus) during exposure to long-term hypoxia. Am J Physiol Regul Integr Comp Physiol 297:R224–R234.

Mitrovic D, Perry SF. 2009. The effects of thermally induced gill remodeling on ionocyte distribution and branchial chloride fluxes in goldfish (carassius auratus). J Exp Biol 212(Pt 6):843–852.

Nilsson GE. 1984. Innervation and pharmacology of the gills. In: Fish physiology. Hoar WS, Randall DJ, editors. Orlando: Academic Press. p.185–227.

Nilsson S, Sundin L. 1998. Gill blood flow control. Comp Biochem Physiol A Mol Integr Physiol 119:137–147.

Pequignot J, Gas N. 1971. Histologic modifications of branchial epithelium following vagotomy in the tench. C R Seances Soc Biol Fil 165:1172–1176.

Perry SF, Payan P, Girard JP. 1984. Adrenergic control of branchial chloride transport in the isolated perfused head of the freshwater trout (*Salmo gairdneri*). J Comp Physiol B Biochem Syst Environ Physiol 154:269–274.

Perry SF, Laurent P. 1989. Adaptational responses of rainbow trout to lowered external NaCl concentration: Contribution of the branchial chloride cell. J Exp Biol 147:147–168.

Perry SF, Shahsavarani A, Georgalis T, Bayaa M, Furimsky M, Thomas SL. 2003. Channels, pumps, and exchangers in the gill and kidney of freshwater fishes: Their role in ionic and acid-base regulation. J Exp Zool A Comp Exp Biol 300:53–62.

Pisam M, Auperin B, Prunet P, Rentier-Delrue F, Martial J, Rambourg A. 1993. Effects of prolactin on *α* and *β* chloride cells in the gill epithelium of the saltwater adapted tilapia, *Oreochromis niloticus*. Anat Rec 235:275–284.

Prunet P, Pisam M, Claireaux JP, Boeuf G, Rambourg A. 1994. Effects of growth hormone on gill chloride cells in juvenile atlantic salmon (l). Am J Physiol 266:R850–R857.

Saltys HA, Jonz MG, Nurse CA. 2006. Comparative study of gill neuroepithelial cells and their innervation in teleosts and *Xenopus* tadpoles. Cell Tissue Res 323:1–10.

Sollid J, De Angelis P, Gundersen K, Nilsson GE. 2003. Hypoxia induces adaptive and reversible gross morphological changes in crucian carp gills. J Exp Biol 206:3667–3673.

Sollid J, Weber RE, Nilsson GE. 2005. Temperature alters the respiratory surface area of crucian carp, *Carassius carassius*, and goldfish, *Carassius auratus*. J Exp Biol 208:1109–1116.

Sundin L, Nilsson S. 2002. Branchial innervation. J Exp Zool 293:232–248.

Thomas S, Fievet B, Claireaux G, Motais R. 1988. Adaptive respiratory responses of trout to acute hypoxia. I. Effects of water ionic composition on blood acid-base status response and gill morphology. Respir Physiol 74:77–89.

Tipsmark CK, Madsen SS, Seidelin M, Christensen AS, Cutler, CP, Cramb, G. 2002. Dynamics of Na^+, K^+, $2Cl^-$

cotransporter and Na$^+$, K$^+$-ATPase expression in the branchial epithelium of brown trout (*Salmo trutta*) and Atlantic salmon (*Salmo salar*). J Exp Zool 293:106–118.

Tipsmark CK, Madsen SS, Borski RJ. 2004. Effect of salinity on expression of branchial ion transporters in striped bass (*Morone saxatilis*). J Exp Zool 301A:979–991.

Trevarrow B, Marks DL, Kimmel CB. 1990. Organization of hindbrain segments in the zebrafish embryo. Neuron 4: 669–679.

Tsai J, Hwang PP. 1998. The wheat germ agglutinin binding sites and development of the mitochondria-rich cells in gills of tilapia (*Oreochromis mossambicus*). Fish Physiol Biochem 19:95–102.

Tzaneva V, Bailey S, Perry SF. 2011. The interactive effects of hypoxemia, hyperoxia and temperature on the gill mor-phology of goldfish (carassius auratus). Am J Physiol Regul Integr Comp Physiol.

Wilson JM, Laurent P, Tufts BL, Benos DJ, Donowitz M, Vogl AW, Randall DJ. 2000. NaCl uptake by the branchial epi-thelium in freshwater teleost fish: an immunological approach to ion-transport protein localization. J Exp Biol 203:2279–2296.

Zaccone G, Ainis L, Mauceri A, Lo Cascio P, Lo Giudice F, Fasulo S. 2003. NANC nerves in the respiratory air sac and branchial vasculature of the Indian catfish, *Hetero-pneustes fossilis*. Acta Histochem 105:151–163.

Zaccone G, Mauceri A, Fasulo S. 2006. Neuropeptides and nitric oxide synthase in the gill and the air-breathing organs of fishes. J Exp Zool A Comp Exp Biol 305:428–439.